J Math Chem
DOI 10.1007/s10910-017-0735-y

ORIGINAL PAPER

Optimal control of multiple two-photon transitions

Dewen Cao[1,2] · **Yaoxiong Wang**[1,2] · **Shouzhi Li**[1,2] · **Ling Yang**[1,2] · **Feng Shuang**[1,2,3] · **Fang Gao**[1]

Received: 1 December 2016 / Accepted: 27 January 2017

Abstract Optimal strategies to maximize the two-photon transition amplitude have been well studied. However, for a system with multiple intermediate states linking the same initial and final states, the question that how to achieve an optimal population transfer remains nontrivial. In this work, we propose a systematic block scheme to maximize the transition amplitude by explicitly considering the interferences among different transition pathways. The scheme can probably provide a quasi-optimal solution, even considering the uncertainties and noises in experiments. Cases with infinitesimal and finite spectral resolution are both investigated. A special example with all first transition frequencies being larger than half of the two-photon transition frequencies is employed to demonstrate our scheme. The analysis provides valuable insights on how to manipulate the interferences in control of quantum systems.

Keywords Quantum control · Pulse shaping · Two-photon transitions · Boundaries analysis · Optimal control

1 Introduction

Two-photon transition is one important physical process in quantum world, and numerous coherent control schemes have been proposed to optimize the transition amplitude

✉ Fang Gao
gaofang@iim.ac.cn

1 Institute of Intelligent Machines, Chinese Academy of Sciences, Hefei 230031, Anhui, China

2 Department of Automation, University of Science and Technology of China, Hefei 230026, Anhui, China

3 Department of Mechanical Engineering, Anhui Polytechnic University, Wuhu 241000, Anhui, China

Published online: 01 February 2017

[1–14]. The $5s \rightarrow 5p \rightarrow 5d$ transition of the rubidium atom can be effectively enhanced by frequency-swept ultrafast laser pulses with both "intuitive" and "counter-intuitive" schemes [1]. Then Silberberg's group investigated the two-photon transition in the frequency domain [2,5] and proposed that a $\pi/2$ step scheme can enhance the amplitude via the constructive interference between resonant and non-resonant terms [5]. Various works have been carried out based on this typical work. Lee *et al.* studied how to achieve the constructive interference between two pathways in a diamond-configuration system with an eight block scheme [10]. We have also compared different coherent control schemes to manipulate the two two-photon transition pathways in atomic rubidium [13], and found that the eight block scheme is a practical scheme for experimental implementation. This block scheme can be further improved by accurately considering the non-resonant terms belonging to each block [15]. To generalize this idea to a system with multiple intermediate states linking the same initial and final states, one has to carefully determine the boundaries of the spectral blocks to achieve maximal constructive interferences among different two-photon transition pathways. A systematic strategy is proposed in this work from this point of view.

The paper is organized as follows. Section 2 gives the theoretical model to describe the transition from the initial state to the target state via N intermediate states. Section 3 shows the optimal control schemes to maximize the transition amplitude with infinitesimal and finite spectral resolution. A specific example is demonstrated in Sect. 4 for illustration. Conclusions are given in Sect. 5.

2 Theoretical model

Multiple two-photon transitions can be involved in a typical system shown in Fig. 1. The initial and final states are, respectively, labeled as $|g\rangle$ and $|f\rangle$, and thus the intermediate states labeled as $|n\rangle$ $(n = 1, 2, \ldots, N)$, indicate N two-photon transitions. According to the second order time-dependent perturbation theory, the sum of the amplitudes of these transitions induced by a weak laser pulse $\varepsilon(t)$ is:

$$U(t) = -\sum_n \frac{\mu_{ng}\mu_{fn}}{\hbar^2} \int_{-\infty}^{t} \mathrm{d}t_1 \int_{-\infty}^{t_1} \mathrm{d}t_2 \varepsilon(t_1)\, \varepsilon(t_2) \exp\left(\mathrm{i}\omega_{fn} t_1\right) \exp\left(\mathrm{i}\omega_{ng} t_2\right), \tag{1}$$

where μ_{fn} and μ_{ng} are the transition dipoles, and $\omega_{ij} = (E_i - E_j)/\hbar$ are the transition frequencies.

For simplicity, we define some abbreviations: $\omega_n = \omega_{ng}$, $\hat{\omega} = \omega_{fg} - \omega$, and $\upsilon_n = \mu_{ng}\mu_{fn}/\hbar^2$. In some cases, dipole moments are real numbers. For example, when a linearly polarized laser is employed in the excitation of atoms, only $\triangle m = 0$ transitions will occur [10,16]. Here m is the magnetic quantum number, and dipole moments are real for this kind of transitions [16]. In the following, we assume all dipole moments are real or have the same phase along different pathways. The final amplitude after the pulse is over (i.e. $t \rightarrow \infty$) can be written as the combination of resonant and non-resonant terms in frequency domain [5]:

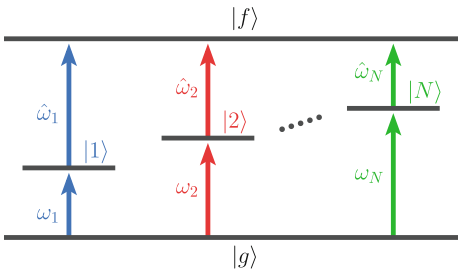

Fig. 1 (Color online) A typical system involving N two-photon transitions. The resonant frequencies are labeled as ω_n for transitions from $|g\rangle$ to $|n\rangle$, and $\hat{\omega}_n$ for those from $|n\rangle$ to $|f\rangle$

$$U = \sum_n U^{(n)} = \sum_n \left[U_r^{(n)} + U_{nr}^{(n)} \right], \tag{2}$$

with

$$U_r^{(n)} = -\pi \upsilon_n E(\omega_n) E\left(\hat{\omega}_n\right), \tag{3}$$

$$U_{nr}^{(n)} = \mathrm{i}\upsilon_n \wp \int_{-\infty}^{\infty} \frac{E(\omega) E\left(\hat{\omega}\right)}{\omega_n - \omega} \mathrm{d}\omega, \tag{4}$$

where $E(\omega)$ is the Fourier transform of $\varepsilon(t)$ and $\wp$ is the Cauchy principal value. The subscripts r and nr denote the resonant and non-resonant parts, respectively.

An Gaussian envelope pulse $E(\omega)$ is modulated to optimize the transition probability from the state $|g\rangle$ to $|f\rangle$ with

$$E(\omega) = b(\omega) G(\omega) \mathrm{e}^{\mathrm{i}\phi(\omega)}, \tag{5}$$

where $G(\omega)$ is the original Gaussian envelope function, and $\phi(\omega)$ (limited within $[-\pi, \pi]$) and $b(\omega)$ (within $[0, 1]$) are the phase and amplitude modulations, respectively.

With the definitions $g(\omega) = G(\omega)G(\hat{\omega})$ and $h(\omega) = b(\omega)b(\hat{\omega})\mathrm{e}^{\mathrm{i}\phi(\omega)}\mathrm{e}^{\mathrm{i}\phi(\hat{\omega})}$, the resonant and non-resonant parts of the two-photon transition labeled with n can be rewritten as

$$U_r^{(n)} = -\pi \upsilon_n h(\omega_n) g(\omega_n), \tag{6}$$

$$U_{nr}^{(n)} = \mathrm{i}\upsilon_n \wp \int_{-\infty}^{\infty} \frac{h(\omega) g(\omega)}{\omega_n - \omega} \mathrm{d}\omega. \tag{7}$$

The fact that $g(\omega)$ and $h(\omega)$ are axis-symmetric about $\omega = \omega_{fg}/2$ leads to $g(\hat{\omega}) = g(\omega)$ and $h(\hat{\omega}) = h(\omega)$. To make our analysis straight forward, it is necessary to rewrite the integration into the region $(\omega_{fg}/2, \infty)$,

$$\begin{aligned} \wp \int_{-\infty}^{\infty} \frac{g(\omega) h(\omega)}{\omega_n - \omega} \mathrm{d}\omega &= \wp \left(\int_{-\infty}^{\omega_{fg}/2} \frac{g(\omega) h(\omega)}{\omega_n - \omega} \mathrm{d}\omega + \int_{\omega_{fg}/2}^{\infty} \frac{g(\omega) h(\omega)}{\omega_n - \omega} \mathrm{d}\omega \right) \\ &= \wp \left(\int_{-\infty}^{\omega_{fg}/2} \frac{g\left(\hat{\omega}\right) h\left(\hat{\omega}\right)}{\omega_n - \hat{\omega}} \mathrm{d}\hat{\omega} + \int_{\omega_{fg}/2}^{\infty} \frac{g(\omega) h(\omega)}{\omega_n - \omega} \mathrm{d}\omega \right) \end{aligned}$$

$$
\begin{aligned}
&= \wp \left(\int_{\omega_{fg}/2}^{\infty} \frac{g(\omega) h(\omega)}{\omega - \hat{\omega}_n} \mathrm{d}\omega + \int_{\omega_{fg}/2}^{\infty} \frac{g(\omega) h(\omega)}{\omega_n - \omega} \mathrm{d}\omega \right) \\
&= \wp \int_{\omega_{fg}/2}^{\infty} g(\omega) h(\omega) \left(\frac{1}{\omega_n - \omega} - \frac{1}{\hat{\omega}_n - \omega} \right) \mathrm{d}\omega. \qquad (8)
\end{aligned}
$$

Here the variable transformation $\omega \to \hat{\omega}$ is used.

Then the total non-resonant amplitude $U_{nr} = \sum_n U_{nr}^{(n)}$ is

$$
U_{nr} = \mathrm{i}\wp \int_{\omega_{fg}/2}^{\infty} g(\omega) h(\omega) f(\omega) \mathrm{d}\omega. \qquad (9)
$$

Here $f(\omega)$ is defined as

$$
f(\omega) = \sum_n \upsilon_n \left(\frac{1}{\omega_n - \omega} - \frac{1}{\hat{\omega}_n - \omega} \right), \qquad (10)
$$

$g(\omega)$ is the amplitude without modulation, and $h(\omega)$ characterizes the modulation effect. To achieve an optimal transition probability, signs of $h(\omega) f(\omega)$ should be the same across the whole frequency domain. So $h(\omega)$ must be carefully chosen according to the sign of $f(\omega)$, which is dominantly determined by the integration near the resonant frequencies ω_n and $\hat{\omega}_n$.

3 Control scheme

3.1 Notations and definitions

The real poles and real zeros of the rational fractional function $f(\omega)$ play an decisive role for our control scheme, because $f(\omega)$ may change signs at these points by which the frequency domain is divided into multiple intervals. The poles of $f(\omega)$ are ω_n and $\hat{\omega}_n$ $(n = 1, 2, \ldots, N)$, and its real zeros are labeled as x_i $(i = 1, 2, \ldots, M)$. Since $f(\omega)$ is axis-symmetric about $\omega = \omega_{fg}/2$, we have $f(\hat{x}_i) = 0$ if $f(x_i) = 0$.

The sets of poles and real zeros are defined as

$$
\begin{aligned}
\mathcal{P} &= \left\{ \omega : \omega = \omega_n \text{ or } \omega = \hat{\omega}_n; n = 1, 2, \ldots, N \right\}, \\
\mathcal{P}_> &= \left\{ \omega : \omega \in \mathcal{P}; \omega \geq \omega_{fg}/2 \right\}. \qquad (11)
\end{aligned}
$$

and

$$
\begin{aligned}
\mathcal{Z} &= \{ x_i; i = 1, 2, \ldots, M \}, \\
\mathcal{Z}_> &= \left\{ x_i : x_i \in \mathcal{Z}; x_i \geq \omega_{fg}/2 \right\}. \qquad (12)
\end{aligned}
$$

A new set $\mathcal{T}$ is introduced by adding the symmetry frequency $\omega_{fg}/2$ and infinity

$$\mathcal{T} = \mathcal{P}_{>} \bigcup \mathcal{Z}_{>} \bigcup \{\omega_{fg}/2, \infty\}. \tag{13}$$

Its elements can be arranged in an ascending order to form a set $\mathcal{T}_o$.

$$\mathcal{T}_o = \{\alpha_1, \alpha_2, \ldots \alpha_i, \ldots, \alpha_{M_o} : \alpha_i < \alpha_{i+1}; \alpha_i, \alpha_{i+1} \in \mathcal{T}\}. \tag{14}$$

Here M_o denotes the number of elements in $\mathcal{T}_o$. It is obvious that the first element $\alpha_1 = \omega_{fg}/2$ and the last element $\alpha_{M_o} = \infty$.

The spectral interval between α_i and α_{i+1} is defined as $\mathcal{A}_i$.

$$\mathcal{A}_i = (\alpha_i, \alpha_{i+1}), \tag{15}$$

where $\alpha_i, \alpha_{i+1} \in \mathcal{T}_o$ and $i = 1, 2, \ldots, M_o - 1$.

The sign function Sgn(x) is

$$\mathrm{Sgn}(x) = \begin{cases} +1 & x > 0, \\ 0 & x = 0, \\ -1 & x < 0. \end{cases} \tag{16}$$

Theorem 3.1 *In each interval* $\mathcal{A}_i$, $\mathrm{Sgn}[f(\omega)]$ *is always the same (*1 *or* -1*). In other words,* $\mathrm{Sgn}[f(\omega_1) f(\omega_2)] = 1$, *if* ω_1 *and* ω_2 *are in the same interval* $\mathcal{A}_i$.

Proof Assume $\mathrm{Sgn}[f(\omega_1) f(\omega_2)] = -1$ (i.e. $f(\omega_1) f(\omega_2) < 0$), when ω_1 and ω_2 be in the same interval $\mathcal{A}_i$. Then $f(\omega)$ must have at least one zero point between ω_1 and ω_2 since $f(\omega)$ is continuous in the interval $\mathcal{A}_i$. It contradicts with the fact that "In any interval $\mathcal{A}_i$, there are no poles and zeros of $f(\omega)$".

As shown in Fig. 2a, the intervals $\{\mathcal{A}_i\}$ can be classified into two types by the sign of $f(\omega)$ ($\omega \in \mathcal{A}_i$). Their combinations are defined as $\mathcal{A}_+$ and $\mathcal{A}_-$.

$$\begin{aligned} \mathcal{A}_+ &= \bigcup_{i=1}^{M_o - 1} \{\mathcal{A}_i : \mathrm{Sgn}[f(\omega)] = +1, \omega \in \mathcal{A}_i\}, \\ \mathcal{A}_- &= \bigcup_{i=1}^{M_o - 1} \{\mathcal{A}_i : \mathrm{Sgn}[f(\omega)] = -1, \omega \in \mathcal{A}_i\}. \end{aligned} \tag{17}$$

□

3.2 Optimization with infinitesimal spectral resolution

Here we assume that the spectral resolution of the pulse is infinitesimal. Hence it is possible to change the pulse phase at any frequency. According to Eqs. (2), (6) and (9), the total transition amplitude is

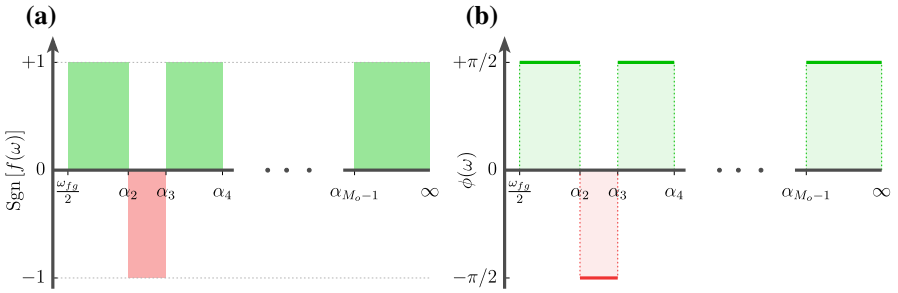

Fig. 2 (Color online) The schematic diagram of Sgn$[f(\omega)]$ and $\phi(\omega)$ versus ω with infinitesimal spectral resolution. Here $\alpha_1, \alpha_2, \ldots, \alpha_i, \ldots, \alpha_{M_o}$ are are the characteristic frequencies in ascending order. **a** In each interval $\mathcal{A}_i$ (i.e. (α_i, α_{i+1})), Sgn$[f(\omega)]$ is always the same (+1 colored with *green* or −1 with *red*). b The optimal phase function $\phi(\omega)$ in Eq. (21) maximizing $|U|$. Within $\mathcal{A}_+$, $\phi(\omega)$ is set to be $+\pi/2$; while in $\mathcal{A}_-$, $\phi(\omega)$ is equal to $-\pi/2$

$$
\begin{aligned}
U =& -\pi \sum_{n=1}^{N} \upsilon_n h(\omega_n) g(\omega_n) + \mathrm{i}\wp \int_{\omega_{fg}/2}^{\infty} g(\omega) h(\omega) f(\omega) \mathrm{d}\omega \\
=& -\pi \sum_{n=1}^{N} \upsilon_n h(\omega_n) g(\omega_n) + \mathrm{i}\wp \int_{\mathcal{A}_- \bigcup \mathcal{A}_+} h(\omega) g(\omega) f(\omega) \mathrm{d}\omega \\
=& -\pi \sum_{n=1}^{N} \upsilon_n h(\omega_n) g(\omega_n) + \mathrm{i}\wp \int_{\mathcal{A}_+} h(\omega) g(\omega) |f(\omega)| \mathrm{d}\omega \\
& - \mathrm{i}\wp \int_{\mathcal{A}_-} h(\omega) g(\omega) |f(\omega)| \mathrm{d}\omega.
\end{aligned} \tag{18}
$$

Since $\upsilon_n > 0$, $g(\omega) > 0$ and $|h(\omega)| \leq 1$, we can easily maximize $|U|$,

$$
|U|_{max} = \pi \sum_{n=1}^{N} \upsilon_n g(\omega_n) + \wp \int_{\omega_{fg}/2}^{\infty} g(\omega) |f(\omega)| \mathrm{d}\omega, \tag{19}
$$

with the following conditions

$$
h(\omega) = \begin{cases} +1 & \omega \in \mathcal{P}_>, \\ -\mathrm{i} & \omega \in \mathcal{A}_-, \\ +\mathrm{i} & \omega \in \mathcal{A}_+. \end{cases} \tag{20}
$$

Then $b(\omega)$ and $\phi(\omega)$ can be obtained according to $h(\omega) = b(\omega) b(\hat{\omega}) \mathrm{e}^{\mathrm{i}\phi(\omega)} \mathrm{e}^{\mathrm{i}\phi(\hat{\omega})}$. Without loss of generality, we assume $b(\omega) = 1$ and $\phi(\omega) = 0$ when $\omega \in (-\infty, \omega_{fg}/2)$, and have

$$
\begin{aligned}
& b(\omega) = 1, \omega \in \left(\omega_{fg}/2, +\infty\right), \\
& \phi(\omega) = \begin{cases} 0 & \omega \in \mathcal{P}_>, \\ -\pi/2 & \omega \in \mathcal{A}_-, \\ +\pi/2 & \omega \in \mathcal{A}_+. \end{cases}
\end{aligned} \tag{21}
$$

The schematic diagram of $\phi(\omega)$ is shown in Fig. 2b.

So there are just three steps in the optimal scheme to maximize $|U|$ when we could modulate the pulse at any frequency with infinitesimal resolution:

Step 1: Determine all poles and zeros of $f(\omega)$, then arrange them in ascending order to form a sequence $\mathcal{T}_o$.

Step 2: Divide the frequency domain greater than $\omega_{fg}/2$ into two types of intervals: $\mathcal{A}_-$ and $\mathcal{A}_+$.

Step 3: Obtain the optimal conditions maximizing $|U|$ according to Eq. (21).

3.3 Optimization with finite spectral resolution

In last section, we assume that we could control the pulse at any frequency. However, in experiments, there should be a limitation. It is only possible to change the phase and amplitude simultaneously in a neighbor around a frequency. The limitation leads to necessary modifications of the optimal scheme in Eq. (21) according to the spectral resolution in experiments.

Assuming that β_i is one of the M_2 elements in $\mathcal{P}_>$, we can define a small deleted neighborhood of the singular point β_i,

$$\mathring{\mathcal{V}}(\beta_i, \delta) = \{\omega : 0 < |\omega - \beta_i| \leq \delta\}, \tag{22}$$

$$\mathring{\mathcal{V}} = \bigcup_{i=1}^{M_2} \mathring{\mathcal{V}}(\beta_i, \delta). \tag{23}$$

Here δ depends on the spectral resolution. Phases and amplitudes are the same within $\mathring{\mathcal{V}}(\beta_i, \delta)$ (i.e. $h(\omega) = h(\beta_i)$ when $\omega \in \mathring{\mathcal{V}}(\beta_i, \delta)$). The non-resonant integration within $\mathring{\mathcal{V}}(\beta_i, \delta)$ can thus be written as

$$\begin{aligned} \mathrm{i}\wp \int_{\beta_i-\delta}^{\beta_i+\delta} h(\omega)\, g(\omega)\, f(\omega)\, \mathrm{d}\omega =& \mathrm{i}h(\beta_i)\, \wp \int_{\mathring{\mathcal{V}}(\beta_i,\delta)} g(\omega)\, f(\omega)\, \mathrm{d}\omega \\ =& \mathrm{i}h(\beta_i)\, U_{\beta_i}. \end{aligned}$$

A new function $J(\omega)$ is defined to distinguish the poles.

$$J(\omega) = \begin{cases} 0 & \omega \notin \mathcal{P}_>, \\ 1 & \omega \in \mathcal{P}_>. \end{cases} \tag{24}$$

And an interval can be defined accordingly.

$$\mathcal{B}_i = (\alpha_i + J(\alpha_i) \cdot \delta, \alpha_{i+1} - J(\alpha_{i+1}) \cdot \delta), \tag{25}$$

with α_i, α_{i+1} defined in Eq. (14).

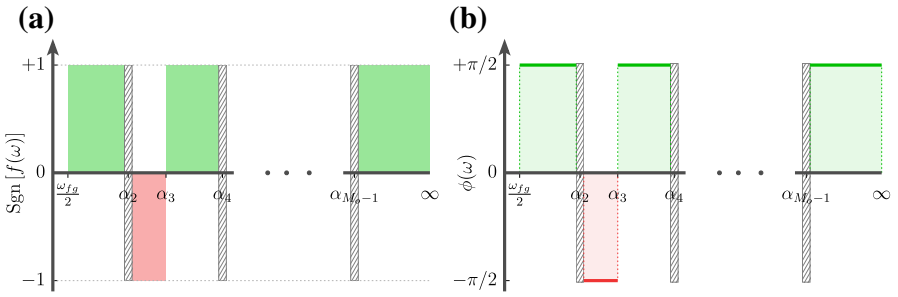

Fig. 3 (Color online) The schematic diagram of Sgn$[f(\omega)]$ and $\phi(\omega)$ versus ω with infinitesimal spectral resolution. Here $\alpha_1, \alpha_2, \ldots, \alpha_i, \ldots, \alpha_{M_o}$ are the characteristic frequencies in ascending order. **a** The intervals are classified into three types: $\mathcal{B}_+$ colored with *green*, $\mathcal{B}_-$ colored with *red*, and $\mathring{\mathcal{V}}(\beta_i, \delta)$ labeled with *gray*. Sgn$[f(\omega)]$ is equal to 1 within $\mathcal{B}_+$ and -1 within $\mathcal{B}_-$. $\mathring{\mathcal{V}}(\beta_i, \delta)$ is a small deleted neighborhood of the poles (e.g. α_2, α_4 and α_{M_0-1}). **b** The optimal phase $\phi(\omega)$ in Eq. (34) maximizing $|U|$. Within $\mathcal{B}_+$ and $\mathcal{B}_-$, $\phi(\omega)$ are set to be $+\pi/2$ and $-\pi/2$ respectively, while in $\mathring{\mathcal{V}}(\beta_i, \delta)$, and $\phi(\omega)$ is equal to θ_i

As shown in Fig. 3a, the intervals $\{\mathcal{B}_i\}$ can also be classified by the sign function.

$$\begin{aligned}\mathcal{B}_- &= \bigcup_{i=1}^{M_2} \{\mathcal{B}_i : \mathrm{Sgn}\,[f(\omega)] = -1, \omega \in \mathcal{B}_i\},\\ \mathcal{B}_+ &= \bigcup_{i=1}^{M_2} \{\mathcal{B}_i : \mathrm{Sgn}\,[f(\omega)] = +1, \omega \in \mathcal{B}_i\}.\end{aligned} \tag{26}$$

To determine the optimal phase within $\mathring{\mathcal{V}}(\beta_i, \delta)$, an identification function $X(\omega, \beta_i)$ is defined.

$$X(\omega, \beta_i) = \begin{cases} 1 & \text{if } (\omega - \beta_i)(\hat{\omega} - \beta_i) = 0, \\ 0 & \text{if } (\omega - \beta_i)(\hat{\omega} - \beta_i) \neq 0. \end{cases} \tag{27}$$

Intervals $\mathcal{B}_-$, $\mathcal{B}_+$ and $\mathring{\mathcal{V}}(\beta_i, \delta)$ all contribute to the sum amplitude U.

$$\begin{aligned}U &= -\pi \sum_{n=1}^{N} \upsilon_n h(\omega_n) g(\omega_n) + \mathrm{i}\wp \int_{\omega_{fg}/2}^{\infty} h(\omega) g(\omega) f(\omega)\, \mathrm{d}\omega\\ &= -\pi \sum_{n=1}^{N} \upsilon_n h(\omega_n) g(\omega_n) + \mathrm{i}\wp \int_{\mathcal{B}_- \bigcup \mathcal{B}_+ \bigcup \mathring{\mathcal{V}}} h(\omega) g(\omega) f(\omega)\, \mathrm{d}\omega\\ &= -\pi \sum_{n=1}^{N} \upsilon_n h(\omega_n) g(\omega_n) + \mathrm{i} \sum_{i=1}^{M_2} h(\beta_i) U_{\beta_i} + \mathrm{i}\wp \int_{\mathcal{B}_- \bigcup \mathcal{B}_+} h(\omega) g(\omega) f(\omega)\, \mathrm{d}\omega\\ &= -\sum_{i=1}^{M_2} h(\beta_i) \left[\pi \sum_{n=1}^{N} X(\omega_n, \beta_i) \upsilon_n g(\omega_n) - \mathrm{i} U_{\beta_i} \right]\\ &\quad + \mathrm{i}\wp \int_{\mathcal{B}_- \bigcup \mathcal{B}_+} h(\omega) g(\omega) f(\omega)\, \mathrm{d}\omega. \end{aligned} \tag{28}$$

The first term contains the non-resonant integration within $\mathring{\mathcal{V}}(\beta_i, \delta)$ and the resonant terms coupling with characteristic frequencies $\{\beta_i\}$, which can be written in the polar coordinate frame.

$$l_i \exp\{-\mathrm{i}\theta_i\} = \pi \sum_{n=1}^{N} X(\omega_n, \beta_i)\, \upsilon_n g(\omega_n) - \mathrm{i}U_{\beta_i},$$

with

$$l_i = \sqrt{\left[\pi \sum\nolimits_{n=1}^{N} X(\omega_n, \beta_i)\, \upsilon_n g(\omega_n)\right]^2 + \left(U_{\beta_i}\right)^2}, \tag{29}$$

$$\tan\theta_i = \frac{U_{\beta_i}}{\pi \sum_{n=1}^{N} X(\omega_n, \beta_i)\, \upsilon_n g(\omega_n)}. \tag{30}$$

Then Eq. (28) becomes

$$\begin{aligned} U &= -\sum_{i=1}^{M_2} h(\beta_i)\, l_i \exp\{-\mathrm{i}\theta_i\} + \mathrm{i}\wp \int_{\mathcal{B}_- \bigcup \mathcal{B}_+} h(\omega)\, g(\omega)\, f(\omega)\, \mathrm{d}\omega \\ &= -\sum_{i=1}^{M_2} h(\beta_i)\, l_i \exp\{-\mathrm{i}\theta_i\} - \mathrm{i}\int_{\mathcal{B}_-} h(\omega)\, g(\omega)\, |f(\omega)|\, \mathrm{d}\omega \\ &\quad + \mathrm{i}\int_{\mathcal{B}_+} h(\omega)\, g(\omega)\, |f(\omega)|\, \mathrm{d}\omega. \end{aligned} \tag{31}$$

Since $l_i > 0$, $g(\omega) > 0$ and $|h(\omega)| \leq 1$, we can easily maximize $|U|$ as

$$|U|_{max} = \sum_{i=1}^{M_2} l_i + \int_{\mathcal{B}_- \bigcup \mathcal{B}_+} g(\omega)\, |f(\omega)|\, \mathrm{d}\omega, \tag{32}$$

when

$$h(\omega) = \begin{cases} \exp\{\mathrm{i}\theta_i\} & \omega \in \mathring{\mathcal{V}}(\beta_i, \delta), \\ -\mathrm{i} & \omega \in \mathcal{B}_-, \\ +\mathrm{i} & \omega \in \mathcal{B}_+. \end{cases} \tag{33}$$

With $h(\omega) = b(\omega)b(\hat{\omega})\mathrm{e}^{\mathrm{i}\phi(\omega)}\mathrm{e}^{\mathrm{i}\phi(\hat{\omega})}$, $b(\omega)$ and $\phi(\omega)$ can be obtained accordingly

$$\begin{aligned} b(\omega) &= 1, \omega \in \left(\omega_{fg}/2, +\infty\right), \\ \phi(\omega) &= \begin{cases} \theta_i & \omega \in \mathring{\mathcal{V}}(\beta_i, \delta), \\ -\pi/2 & \omega \in \mathcal{B}_-, \\ +\pi/2 & \omega \in \mathcal{B}_+. \end{cases} \end{aligned} \tag{34}$$

Without losing generality, we assume $b(\omega) = 1$ and $\phi(\omega) = 0$ when $\omega \in (-\infty, \omega_{fg}/2)$.

The schematic diagram of $\phi(\omega)$ is shown in Fig. 3b. It is noted that $\theta_i = \mathrm{O}(\delta)$ according to Eq. (30), since $U_{\beta_i} = \int_{\mathring{\mathcal{V}}(\omega_n,\beta_i)} g(\omega) f(\omega) \mathrm{d}\omega = \mathrm{O}(\delta)$. Thus θ_i equals to zero approximately, when δ is small enough.

So there are four steps in the optimal scheme to maximize $|U|$ with finite spectral resolution:

Step 1: Determine all poles and zeros of $f(\omega)$, then arrange them in ascending order to form a sequence $\mathcal{T}_o$.

Step 2: According to the spectral resolution in experiments, specify δ and $\mathring{\mathcal{V}}(\beta_i, \delta)$.

Step 3: Divide the frequency domain greater than $\omega_{fg}/2$ into three types of intervals: $\mathcal{B}_-$, $\mathcal{B}_+$ and $\mathring{\mathcal{V}}$.

Step 4: Obtain the optimal conditions maximizing $|U|$ according to Eq. (34).

4 Optimal control of a special system

In this section, we consider the optimal control of a special system with multiple two-photon transitions. The system has the structure as shown in Fig. 1, but all of its first transition frequencies, $\omega_1, \omega_2, \ldots, \omega_N$, are larger than $\omega_{fg}/2$. Without loss of generality, we assume $\omega_{fg}/2 < \omega_1 < \omega_2 < \cdots < \omega_N$. We will prove that, for this special system, all zeros of Eq. (10) are real. This property makes the control scheme of this system quite simple.

Equation (10) can be rewritten as

$$\begin{aligned} f(\omega) &= \sum_{n=1}^{N} \frac{\upsilon_n \left(\hat{\omega}_n - \omega_n\right)}{(\omega_n - \omega)\left(\hat{\omega}_n - \omega\right)} \\ &= \frac{f_{up}(\omega)}{f_{dw}(\omega)}, \end{aligned} \tag{35}$$

with

$$\begin{aligned} f_{up}(\omega) &= \sum_{n=1}^{N} \lambda_n \left\{ \prod_{i=1; i\neq n}^{N} (\omega - \omega_i)\left(\omega - \hat{\omega}_i\right) \right\}, \\ f_{dw}(\omega) &= \prod_{n=1}^{N} (\omega - \omega_n)\left(\omega - \hat{\omega}_n\right), \\ \lambda_n &= \upsilon_n \left(\hat{\omega}_n - \omega_n\right). \end{aligned} \tag{36}$$

Here $f_{up}(\omega)$ is a $2(N-1)$ degree real-polynomial, with the coefficient of $\omega^{2(N-1)}$ being $\sum_{n=1}^{N} \lambda_n$. It is continuous in the whole frequency domain (i.e. $(-\infty, \infty)$) and axis-symmetric about $\omega = \omega_{fg}/2$.

The set $\mathcal{P}_>$ for this special system is

$$\mathcal{P}_> = \{\omega_1, \omega_2, \ldots, \omega_N\}. \tag{37}$$

We have

$$f_{up}\left(\omega_I\right) = \lambda_I \prod_{i=1;i\neq I}^{N} \left(\omega_I - \omega_i\right)\left(\omega_I - \hat{\omega}_i\right), \tag{38}$$

which leads to

$$\mathrm{Sgn}\left[f_{up}\left(\omega_I\right)\right] = (-1)^{N-I+1}, I = 1, 2, \ldots, N. \tag{39}$$

It is easy to obtain $\mathrm{Sgn}[f(\omega_I) f(\omega_{I+1})] = -1$. Since $f_{up}(\omega)$ is continuous, there are at least one real root between ω_I and ω_{I+1} for $f_{up}(\omega) = 0$. The axis-symmetric feature of $f_{up}(\omega)$ leads to the fact that there are also at least one real root in the interval $(\hat{\omega}_{I+1}, \hat{\omega}_I)$. Therefore, there are totally at least $2(N-1)$ real roots. As known from fundamental theorem of algebra, every non-zero, single-variable, degree n polynomial with complex coefficients has, counted with multiplicity, exactly n roots. So $f_{up}(\omega) = 0$ has $2(N-1)$ roots, and it will just have $2(N-1)$ real roots, with only one real root in each interval (ω_I, ω_{I+1}) or $(\hat{\omega}_{I+1}, \hat{\omega}_I)$.

$\mathcal{Z}_>$ and $\mathcal{T}_o$ are

$$\mathcal{Z}_> = \{x_1, x_2, \ldots, x_{N-1}\}, \tag{40}$$

$$\mathcal{T}_o = \left\{\omega_{fg}/2, \omega_1, x_1, \ldots, \omega_{N-1}, x_{N-1}, \omega_N, \infty\right\}, \tag{41}$$

with x_i being the real root in the interval (ω_I, ω_{I+1}), which is certainly larger than $\omega_{fg}/2$.

The sign of $f(\omega)$ can be determined systematically. For instance, according to Eq. (10), when $\omega \in (x_i, \omega_{i+1})$, we have

$$\begin{aligned}\mathrm{Sgn}\left[f\left(\omega\right)\right] &= \mathrm{Sgn}\left[\lim_{\omega\to\omega_{i+1}^{-}} f\left(\omega\right)\right] \\ &= \mathrm{Sgn}\left[\lim_{\omega\to\omega_{i}^{-}} \frac{1}{\omega_{i+1} - \omega}\right] \\ &= +1.\end{aligned} \tag{42}$$

Similarly, when $\omega \in (\omega_i, x_i)$, we have

$$\begin{aligned}\mathrm{Sgn}\left[f\left(\omega\right)\right] &= \mathrm{Sgn}\left[\lim_{\omega\to\omega_{i}^{+}} f\left(\omega\right)\right] \\ &= \mathrm{Sgn}\left[\lim_{\omega\to\omega_{i}^{+}} \frac{1}{\omega_{i} - \omega}\right] \\ &= -1.\end{aligned} \tag{43}$$

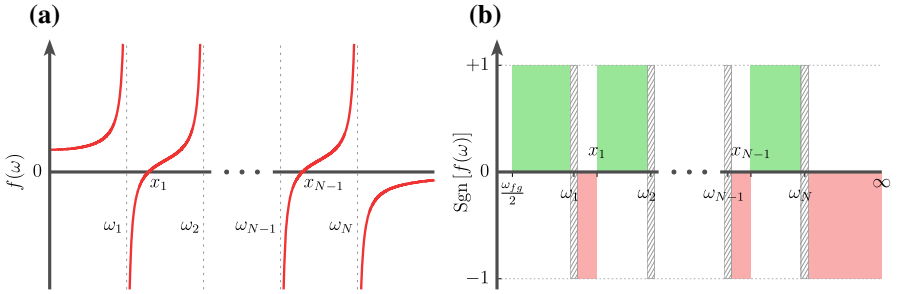

Fig. 4 (Color online) The schematic diagram of $f(\omega)$ and the three types of intervals for the specific system. **a** $f(\omega)$ is larger than zero in each of the intervals $(\omega_{fg}/2, \omega_1)$ and (x_i, ω_{i+1}). In the other intervals, it is less than zero. $\{\omega_1, \omega_2, \ldots, \omega_N\}$ are the poles and $\{x_1, x_2, \ldots, x_{N-1}\}$ are the zeros. **b** Within the intervals $\mathcal{B}_+$ (*green color*), $f(\omega) > 0$; while in $\mathcal{B}_-$ (*red color*), $f(\omega) < 0$. $\mathring{\mathcal{V}}$ consists of N *gray regions*, with each corresponds to a deleted neighborhood of a pole point

Therefore, $f(\omega)$ changes its sign at its poles and zeros, which is clearly shown in Fig. 4a. The three types of intervals can be determined as

$$\begin{aligned}
\mathring{\mathcal{V}} &= \bigcup_{i=1}^{N} \mathring{\mathcal{V}}(\omega_i, \delta)\,, \\
\mathcal{B}_+ &= \left(\omega_{fg}/2, \omega_1 - \delta\right) \bigcup \left[\bigcup_{i=1}^{N-1} (x_i, \omega_{i+1} - \delta)\right], \\
\mathcal{B}_- &= \left[\bigcup_{i=1}^{N-1} (\omega_i + \delta, x_i)\right] \bigcup (\omega_N + \delta, \infty)\,.
\end{aligned} \tag{44}$$

The optimal phases of these intervals can be obtained according to Eq. (34).

Numerical simulation is demonstrated by a five-level system shown in Fig. 5. The laser field is assumed as a Gaussian envelope.[1]

$$G(\omega) = b_0 \exp\left\{-\frac{(\omega - \omega_0)^2}{2\Delta^2}\right\}. \tag{45}$$

The simulation results are listed in Table 1 which shows an enhancement of 6.8 times in the two-photon transitions compared with the transform limited (TL) pulse.

[1] The parameters of the five level system are $\upsilon_1 = 1.1590$, $\upsilon_2 = 1.1615$, $\upsilon_3 = 1.2508$, $\omega_1 = 0.059\,50$, $\omega_2 = 0.060\,10$, $\omega_3 = 0.060\,70$, $\omega_{fg} = 0.1180$ and $\delta = 10^{-9}$. The parameters of laser pulse are $\omega_0 = 0.05826$, $\Delta = 0.001423$ and $b_0 = 0.0006$. Here b_0 is a constant which small enough to make sure that the light-matter interaction is perturbative. The parameters above all use atomic unit.

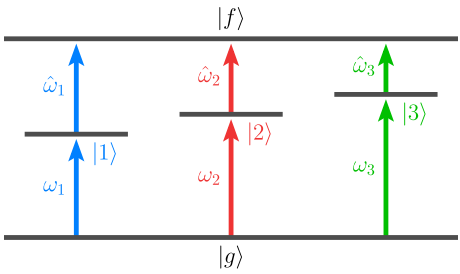

Fig. 5 (Color online) The schematic diagram of a five-level system with $\omega_{fg}/2 < \omega_1 < \omega_2 < \omega_3$

Table 1 Two-photon transition amplitudes of the five-level system in Fig. 5

Control scheme	U_r	U_{nr}	U	$\lvert U\rvert$
TL pulse	-4.723	$4.409i$	$-4.723 + 4.409$i	6.461
Optimal pulse	-4.723	-39.302	-44.025	44.025

The TL pulse means no pulse shaping (i.e. $b(\omega) = 1$, $\phi(\omega) = 0$). The optimal pulse scheme is shown like Fig. 4b. For simplicity, all the values are reduced by a factor of b_0^2

5 Conclusions and discussions

The optimal control of multiple two-photon transitions is investigated in this work. Via the boundaries analysis of Silberberg's expression [5], the optimal control scheme is determined step by step accurately. For experimental consideration, the whole frequency domain is divided into different types of spectral intervals according to the real poles and zeros of $f(\omega)$ and the spectral resolution. The scheme is optimal because it tries to achieve the maximal interferences between different transition terms under experimental spectral resolution consideration. A special case with all the transition frequencies from the initial state to the intermediate states are larger than half of the transition from the initial to final state is employed for demonstration. Due to its special energy level structure, the number of zeros and the sign of $f(\omega)$ in each spectral interval can be determined analytically. Numerical simulation shows that a rather good effect can be achieved with this scheme.

The optimal control of multiple two-photon transitions can be achieved in experiments approximately with our strategy. The key step is to determine the spectral boundaries, around which the phase changes its value. The boundaries include the poles and real zeros of the rational fractional function $f(\omega)$. For a system with N intermediate states, the boundaries include N poles, which are the resonant transition frequencies and can be measured as spectral peaks by sweeping a spectral π-phase step [10], at most $N-1$ real zeros, and half of the transition from the initial state to the target state. So the number of spectral blocks in our strategy is $2 * N$ at most, which means that the complexity of our phase-modulating strategy increases linearly with the number of pathways. Besides, the real zeros only depends on the ratio of transition dipoles along different pathways, not on their absolute values. The case of $N = 2$ can be seen as an accurate version of the scheme proposed in Ref. [10] (i.e. the real zeros are determined more accurately in our scheme), which has proven its effectiveness in

the quantum interference control of atomic Rb. Both the two schemes have four phase variables and thus have the same implementation complexity. Therefore, our strategy can probably provide a quasi-optimal solution, even considering the uncertainties and noises in experiments.

Acknowledgements The authors acknowledge support by the National Natural Science Foundation of China (Grants No. 61203061, No. 61403362, 61374091, and No. 61473199). F Shuang thanks the Leader talent plan of the Universities in Anhui Province for their support.

References

1. B. Broers, H.V.L. van den Heuvell, L.D. Noordam, Efficient population transfer in a three-level ladder system by frequency-swept ultrashort laser pulses. Phys. Rev. Lett. **69**, 2062–2065 (1992)
2. Doron Meshulach, Yaron Silberberg, Coherent quantum control of two-photon transitions by a femtosecond laser pulse. Nature **396**(6708), 239–242 (1998)
3. Doron Meshulach, Yaron Silberberg, Coherent quantum control of multiphoton transitions by shaped ultrashort optical pulses. Phys. Rev. A **60**, 1287–1292 (1999)
4. A.M. Weiner, Femtosecond pulse shaping using spatial light modulators. Rev. Sci. Instrum. **71**(5), 1929–1960 (2000)
5. Nirit Dudovich, Barak Dayan, Sarah M. Gallagher Faeder, Yaron Silberberg, Transform-limited pulses are not optimal for resonant multiphoton transitions. Phys. Rev. Lett. **86**, 47–50 (2001)
6. T. Flissikowski, A. Betke, I.A. Akimov, F. Henneberger, Two-photon coherent control of a single quantum dot. Phys. Rev. Lett. **92**, 227401 (2004)
7. P. Panek, A. Becker, Dark pulses for resonant two-photon transitions. Phys. Rev. A **74**, 023408 (2006)
8. C. Matthew, Stowe, Avi Pe'er, Jun Ye, Control of four-level quantum coherence via discrete spectral shaping of an optical frequency comb. Phys. Rev. Lett. **100**, 203001 (2008)
9. Shian Zhang, Hui Zhang, Tianqing Jia, Zugeng Wang, Zhenrong Sun, Coherent control of two-photon transitions in a two-level system with broadband absorption. Phys. Rev. A **80**, 043402 (2009)
10. Han-gyeol Lee, Hyosub Kim, Jongseok Lim, Jaewook Ahn, Quantum interference control of a four-level diamond-configuration quantum system. Phys. Rev. A **88**, 053427 (2013)
11. Jing Ma, Wenjing Cheng, Shian Zhang, Donghai Feng, Tianqing Jia, Zhenrong Sun, Jianrong Qiu, Coherent quantum control of two-photon absorption and polymerization by shaped ultrashort laser pulses. Laser Phys. Lett. **10**(8), 085304 (2013)
12. Fang Gao, Roberto Rey-de Castro, Ashley M. Donovan, Jian Xu, Yaoxiong Wang, Herschel Rabitz, Feng Shuang, Pathway dynamics in the optimal quantum control of rubidium: cooperation and competition. Phys. Rev. A **89**, 023416 (2014)
13. Fang Gao, Yaoxiong Wang, Roberto Rey-de Castro, Herschel Rabitz, Feng Shuang, Quantum control and pathway manipulation in rubidium. Phys. Rev. A **92**, 033423 (2015)
14. Fang Gao, Yaoxiong Wang, Dewen Cao, Feng Shuang, Coherent control of multiple 2nd-order quantum pathways. Chin. J. Chem. Phys **28**(4), 426–430 (2015)
15. Dewen Cao, Ling Yang, Yaoxiong Wang, Feng Shuang, Fang Gao, Controlling pathway dynamics of a four-level quantum system with pulse shaping. J. Phys. A Math. Theor. **49**(28), 285302 (2016)
16. Z. Ficek, M.R. Wahiddin, *Quantum Optics for Beginners* (CRC Press, Boca Raton, 2014), pp. 21–23